RSC Advances

RSC Publishing

COMMUNICATION

# High performance NIR fluorescent silica nanoparticles for bioimaging†

Cite this: *RSC Advances*, 2013, **3**, 9171

Received 12th March 2013,
Accepted 22nd April 2013

DOI: 10.1039/c3ra41199k

www.rsc.org/advances

Tânia Ribeiro,‡ Sebastian Raja,‡ Ana Sofia Rodrigues, Fábio Fernandes, José Paulo S. Farinha* and Carlos Baleizão*

**We synthesized a new alkoxysilane-functionalized perylenediimide (PDI) dye with fluorescence emission in the near infrared (NIR). Incorporation of the dye into silica nanoparticles and subsequent internalization in living cells shows promising results for application in confocal laser scanning microscopy, allowing simultaneous imaging with other commonly used dyes or fluorescent proteins.**

The higher tissue penetration,[1] lower biological autofluorescence,[2] and reduced light scattering of near infrared (NIR) light (750–1400 nm) have greatly increased the interest in NIR fluorescent dyes for use in chemical biology.[3] Additionally, NIR dyes require only inexpensive laser excitation for use in laser scanning microscopy. However, only a limited number of NIR dyes are readily available, and from those, most are not easily functionalized or are too expensive to allow routine functionalization. Examples of known NIR dyes include cyanines, BODIPYs and squaraines.[4,5] A commonly reported problem of these dyes is their low solubility in water, leading to dye aggregation and undesired changes in the photophysical properties. Although some NIR cyanine dyes have high molar absorptivity, bright fluorescence and good photostability, their functionalization is all but straightforward.[6]

One way to improve the photophysical and photochemical properties of NIR probes is to incorporate them in nanoparticle (NP) supports. The characteristics of NP-based imaging agents such as the ability to carry large molecular payloads and multiple surface targeting groups, together with the possibility to tune their pharmacokinetics, have motivated the development of different systems for use in combined diagnostic and therapeutic (theranostic) applications.[7] Silica nanoparticles (SiNPs) in particular, have been used as supports or carriers for drug delivery,[8] imaging[9] or nanomedicine,[10] due to the possibility of tuning their diameter and pore size, loading drugs, fluorophores or other molecules, and functionalize their surface.[11] The covalent incorporation of NIR dyes in SiNPs, however, have been scarcely reported, and most often require laborious protocols.[12,13]

Perylenediimides (PDIs) are versatile dyes with interesting photophysical properties, such as near-unity fluorescence quantum yield, excitation in the visible region, high photochemical stability and high electron mobility.[14] These properties can be modulated by introduction of substituents in the imide group (affecting the solubility or allowing their immobilization) or in the perylene core (affecting the electronic and optical properties).[15] PDIs have applications in many fields, from photovoltaics to imaging, *etc.*[16,17]

The incorporation of PDIs in nanoparticles can further increase their performance and broaden their application range. The recent incorporation of PDI **1** (Fig. 1) in silica nanoparticles for use in confocal laser scanning microscopy (CLSM) is revealing of the importance of this type of materials.[18–20] However, the emission of PDI **1** falls in the same region (530–600 nm) as most of the dyes presently used for fluorescence imaging (including most fluorescent proteins),[21] and its use in CLSM requires excitation by (expensive) lasers in the region 450–530 nm. The new PDI dye presented here (PDI **2**, Fig. 1) overcomes this problem, featuring excitation in the red region of the spectrum and fluorescence

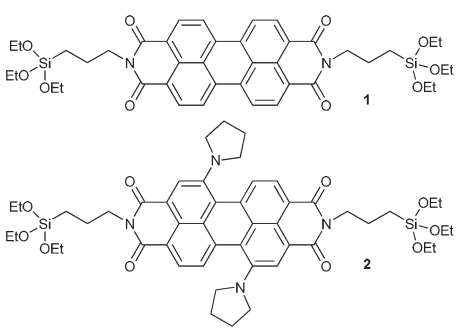


**Fig. 1** Chemical structure of PDI **1** and PDI **2**.

*Centro de Química-Física Molecular and Institute of Nanoscience and Nanotechnology, Instituto Superior Técnico, Universidade Técnica de Lisboa, Av. Rovisco Pais, 1049-001 Lisboa, Portugal. E-mail: farinha@ist.utl.pt; carlos.baleizao@ist.utl.pt*

† Electronic supplementary information (ESI) available: Synthesis and characterization of PDI **2** and **2-SiNP**, and photophysical and confocal data. See DOI: 10.1039/c3ra41199k

‡ T.R. and S.R. have contributed equally to this work.

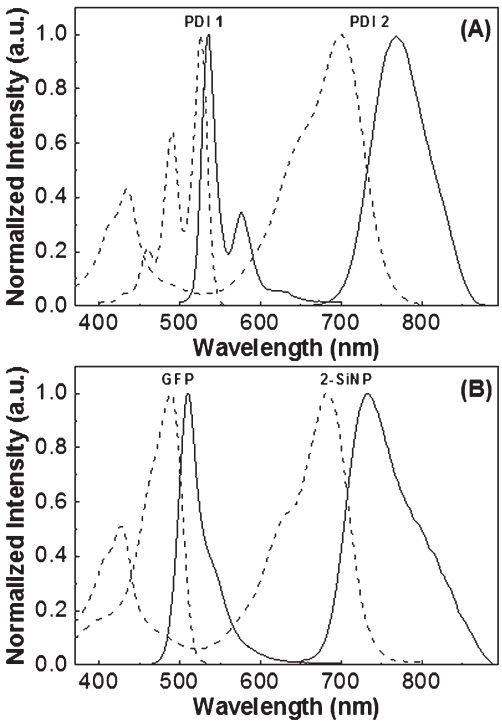


**Fig. 2** (A) Normalized absorption (dashed curve) and fluorescence (solid curve) spectra of PDI **1** and PDI **2** in ethanol. (B) The normalized excitation (dashed curve) and emission (solid curve) spectra of **2-SiNP** in dioxane (in which light scattering is residual) do not overlap with the GFP spectra in water, thus allowing simultaneous imaging of both dyes.

emission in the NIR. It also has alkoxysilane groups in its structure for incorporation in silica nanostructures thus showing great potential for fluorescence microscopy bioimaging.

Our target molecule, PDI **2** (Fig. 1), has propyltriethoxysilane groups in the imide region and two electron-donating pyrrolidine substituents in the perylene core. The triethoxysilane moieties can be used to incorporate the dye in the silica network during the preparation of SiNPs, while the electron-donating substituents shift the fluorescence excitation and emission bands to longer wavelengths than those of PDI **1**. PDI **2** was synthesized by reaction of (3-amino-propyl)triethoxysilane (APTES) with the 1,7-dipyrrolidinylperylene bisanhydride (ESI† for details).[22]

The photophysical properties of PDI **2**, in particular the absorption and fluorescence emission spectra, are dramatically different from those of PDI **1** (Fig. 2A). The absorption and fluorescence emission maxima are 150–200 nm red shifted relative to PDI **1**, and the Stokes shift increases to 40–70 nm depending on the solvent (Fig. 2A, ESI†).

The fluorescence emission spectra of PDI **2** are similar in toluene and dioxane, with maximum emission wavelengths at 724 nm and 728 nm, respectively. However, the wavelength of maximum emission increases to 770 nm in ethanol, leading us to expect similar values for the maximum emission wavelength in water, after encapsulation of PDI **2** in SiNPs. The molar absorptivities at the absorption maximum are similar in all solvents (around 40 000 $M^{-1}$ $cm^{-1}$), and the brightness (the product of the absorptivity and the fluorescence quantum yield) is higher than 10 000 $M^{-1}$ $cm^{-1}$ in most tested solvents (with the exception of ethanol, in which PDI **2** has a lower quantum yield, Table S1, ESI†).

The incorporation of target molecules in SiNPs can be done by physical entrapment inside the core,[23] by surface modification or by covalent attachment to the silica network during the synthesis (using molecules functionalized with alkoxysilane groups).[24] Additionally, post-synthesis surface functionalization can be used to encapsulate the particles in a shell or to immobilize polymers or biomolecules for biotargeting.[25] Another important advantage of incorporating dyes in SiNPs, especially when laser excitation is used, is the oxygen shielding effect that enhances their photostability (the oxygen concentration inside the SiNPs is lower than in most solvents).[26]

We obtained new hybrid fluorescent silica nanoparticles (**2-SiNP**) by encapsulation of PDI **2** using the Stöber method.[27] The two terminal triethoxysilyl groups of PDI **2** were used as a secondary silica source to incorporate the dye in the silica network. The size of the fluorescent nanoparticles, characterized by transmission electron microscopy (TEM) and dynamic light scattering (DLS), was tuned to the optical resolution of CLSM, with the average nanoparticle diameter recovered from TEM equal to 300 nm, and low size dispersity (Fig. S4 and S5, ESI†).

The photophysics of **2-SiNP** is very similar to that of free PDI **2**, showing identical excitation/emission spectra and fluorescence lifetime in several solvents (Fig. 2B and Table S2, ESI†). The photostability of free PDI **2** and **2-SiNP** was compared against DiIC18(5), a carbocyanine Cy5 derivative used in biolabeling. After 2 h of continuous irradiation at $\lambda_{exc}$ = 615 nm using a 450 W Xe lamp, the fluorescence intensity of the DiIC18(5) drops *ca.* 9%, while no change is detected for PDI **2** (Fig. S6, ESI†). The same result was obtained for a dispersion of **2-SiNP** in 1,4-dioxane under the same conditions.

One advantage of using dyes encapsulated in nanoparticles is that the nanoparticles are easily dispersed in solvents where the free dye is insoluble and therefore unusable. In the present case, the water insoluble PDI **2** dye can be used in water after encapsulation in **2-SiNP**. In fact, the wavelength at the emission maximum of **2-SiNP** in water is one of the highest recorded in our study (764 nm, Table S2 in the ESI†). The **2-SiNP** can be excited in a large wavelength range (600–750 nm), and it was possible to obtain CLSM images of the particles in a film using a low power HeNe (633 nm) laser (Fig. S7, ESI†).

The properties of **2-SiNP** encouraged us to evaluate its performance as an *in cellulo* marker for CLSM. The fluorophore excitation in the red and emission in the NIR allow the simultaneous use of more conventional dyes in multicolor imaging systems, an especially interesting characteristic for cells with transfected/expressed GFP or other fluorescent proteins.[21] In Fig. 2B we show the fluorescence excitation and emission spectra of **2-SiNP** (in dioxane, a low polarity solvent known to exhibit physical characteristics close to those of biological micro-environments)[28] and GFP in aqueous solution, with the wavelength range used for GFP imaging falling in the region of minimum absorption and no emission by **2-SiNP**.

 

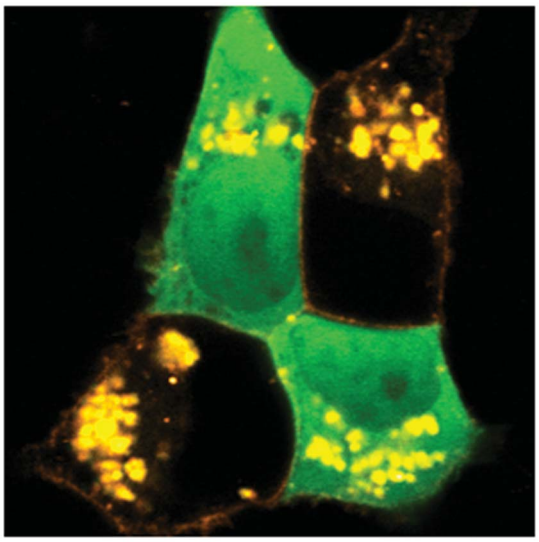

**Fig. 3** CLSM image of HEK293 cells stained with the AF594-WGA plasma membrane marker (orange). GFP in transfected cells is shown in green. The **2-SiNP**, shown in yellow, appear dispersed in the cytosol.

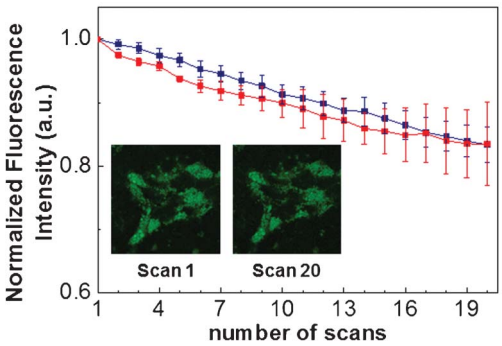


**Fig. 4** Fluorescence intensity of **2-SiNP** (red) and DiIC18(7) membrane marker (blue) in stained HEK293 cells (imaged by CLSM with a 0.325 mW HeNe 633 nm laser, over a set of 20 scans, at 5.12 s per scan). The error bars were determined from 3 different experiments. The fluorescence intensity was obtained by integrating the 645–790 nm wavelength range. The insets are CLSM images of the HEK293 cells loaded with **2-SiNP** obtained at scan 1 and scan 20 (images size 48.75 × 48.75 μm).

HEK293 cells were transfected with free GFP and **2-SiNP** were internalized with a non-optimized protocol. Shortly before imaging, these cells were co-stained with a plasma membrane marker (AF594-WGA). CLSM images show that **2-SiNP** was efficiently internalized in the cells, appearing well dispersed or in small aggregates in the cytosol (Fig. 3). In both cases, **2-SiNP** easily stands out even in GFP transfected cells.

The photostability of **2-SiNP** was compared with that of a commercial NIR membrane marker Cy7 derivative, DiIC18(7), which features an excitation maximum around 750 nm and emission maximum around 780 nm.[29] The HEK293 cells were loaded with either **2-SiNP** or DiIC18(7) using a non-optimized protocol. The fluorescence intensity was measured in CLSM images (integrating the 645–800 nm wavelength range), obtained with a HeNe 633 nm laser as excitation source (with 0.325 mW power, measured at the sample surface). Consecutive images were collected (5.12 s per scan) and the integrated fluorescence intensity evolution is shown in Fig. 4. The fluorescence intensity of **2-SiNP** matches that of DiIC18(7), decreasing only 17% after 20 scans.

Finally, the NIR fluorescent nanoparticles shown here can be easily surface modified for targeting and increased biocompatibility,[30] providing an excellent platform for fluorescence microscopy bioimaging, where several markers are often used simultaneously.

In conclusion, our new PDI dye with alkoxysilane groups for incorporation onto silica nanostructures can be excited in the red, emitting in the NIR. As a proof of concept, the dye was incorporated in silica nanoparticles, which were internalized in HEK293 cells. This showed that the new NIR fluorescent nanoparticles can be used as a platform for *in cellulo* bioimaging applications, even in cells expressing high levels of fluorescent proteins and/or co-stained with different fluorescent dyes. Additionally, the photostability of the dye, either free or encapsulated in SINPs, matches that of the best commercially available NIR markers. We believe these fluorescent nanoparticles have the potential to be a breakthrough in laser scanning microscopy imaging, overcoming the current lack of low cost efficient NIR dyes, while offering the possibility of surface functionalization for targeting and biocompatibilization.

## Acknowledgements

This work was partially supported by Fundação para a Ciência e a Tecnologia (FCT-Portugal) and COMPETE (FEDER) within projects PTDC/CTM/101627/2008 and PTDC/CTM-NAN/2354/2012. T.R., A.S.R., R.S. and F.F. also thank FCT for Ph.D. (SFRH/BD/64702/2009; SFRH/BD/89615/2012) and Pos-Doc (SFRH/BPD/71249/2010; SFRH/BPD/64320/2009) grants. The authors thank Dr Aleksander Fedorov (CQFM-IN) for technical assistance with the picosecond lifetime decay measurements.

## Notes and references

1 R. Weissleder, *Nat. Biotechnol.*, 2001, **19**, 316.
2 S. Boumaza, S. M. Arribas, M. Osborne-Pellegrin, J. C. McGrath, S. Laurent, P. Lacolley and P. Challande, *Hypertension*, 2001, **37**, 1101.
3 S. A. Hilderbrand and R. Weissleder, *Curr. Opin. Chem. Biol.*, 2010, **14**, 71.
4 J. O. Escobedo, O. Rusin, S. Lim and R. M. Strongin, *Curr. Opin. Chem. Biol.*, 2010, **14**, 64.
5 V. J. Pansare, S. Hejazi, W. J. Faenza and R. K. Prud'homme, *Chem. Mater.*, 2012, **24**, 812.
6 M. Panigrahi, S. Dash, S. Patel and B. K. Mishra, *Tetrahedron*, 2012, **68**, 781.
7 K. Y. Choi, G. Liu, S. Lee and X. Chen, *Nanoscale*, 2012, **4**, 330.
8 B. G. Trewyn, I. I. Slowing, S. Giri, H.-T. Chen and V. S.-Y. Lin, *Acc. Chem. Res.*, 2007, **40**, 846.
9 J. Kim, Y. Piao and T. Hyeon, *Chem. Soc. Rev.*, 2009, **38**, 372.
10 S. W. Bae, W. Tan and J.-I. Hong, *Chem. Commun.*, 2012, **48**, 2270.
11 S. Bonacchi, D. Genovese, R. Juris, M. Montalti, L. Prodi, E. Rampazzo and N. Zaccheroni, *Angew. Chem., Int. Ed.*, 2011, **50**, 4056.

12 J. F. Bringley, T. L. Penner, R. Wang, J. F. Harder and W. J. Harrison, *J. Colloid Interface Sci.*, 2008, **320**, 132.
13 E. Herz, H. Ow, D. Bonner, A. Burnsa and U. Wiesner, *J. Mater. Chem.*, 2009, **19**, 6341.
14 X. Zhan, A. Facchetti, S. Barlow, T. J. Marks, M. A. Ratner, M. R. Wasielewski and S. R. Marder, *Adv. Mater.*, 2011, **23**, 268.
15 C. Huang, S. Barlow and S. R. Marder, *J. Org. Chem.*, 2011, **76**, 2386.
16 T. Weil, T. Vosch, J. Hofkens, K. Peneva and K. Müllen, *Angew. Chem., Int. Ed.*, 2010, **49**, 9068.
17 C. Li and H. Wonneberger, *Adv. Mater.*, 2012, **24**, 613.
18 T. Ribeiro, C. Baleizão and J. P. S. Farinha, *J. Phys. Chem. C*, 2009, **113**, 18082.
19 J. Blechinger, R. Herrmann, D. Kiener, F. J. García-García, C. Scheu, A. Reller and C. Bräuchle, *Small*, 2010, **6**, 2427.
20 H. Wang, K. Schaefer, A. Pich and M. Moeller, *Chem. Mater.*, 2011, **23**, 4748.
21 N. C. Shaner, P. A. Steinbach and R. Y. Tsien, *Nat. Methods*, 2005, **2**, 905.
22 F. Wurthner, V. Stepanenko, Z. Chen, C. R. Saha-Moller, N. Kocher and D. Stalke, *J. Org. Chem.*, 2004, **69**, 7933.
23 J. Yan, M. C. Estevez, J. E. Smith, K. Wang, X. He, L. Wang and W. Tan, *Nano Today*, 2007, **2**, 44.
24 F. Hoffmann, M. Cornelius, J. Morell and M. Froba, *Angew. Chem., Int. Ed.*, 2006, **45**, 3216.
25 Y. Gong and F. M. Winnik, *Nanoscale*, 2012, **4**, 360.
26 G. Yao, L. Wang, Y. Wu, J. Smith, J. Xu, W. Zhao, E. Lee and W. Tan, *Anal. Bioanal. Chem.*, 2006, **385**, 518.
27 W. Stöber, A. Fink and E. J. Bohn, *J. Colloid Interface Sci.*, 1968, **26**, 62.
28 N. I. Zahid, O. K. Abou-Zied, R. Hashim and T. Heidelberg, *J. Phys. Chem. C*, 2011, **115**, 19805.
29 I. Texier, M. Goutayer, A. Silva, L. Guyon, D. Djaker, V. Josserand, E. Neumann, J. Bibette and F. Vinet, *J. Biomed. Opt.*, 2009, **14**, 054005.
30 H. Jaganathan and B. Godin, *Adv. Drug Delivery Rev.*, 2012, **64**, 1800.

 